Journal of proteome research

Article

pubs.acs.org/jpr

Metabolomic Analysis of the Effects of Chronic Arsenic Exposure in a Mouse Model of Diet-Induced Fatty Liver Disease

Xue Shi,[†] Xiaoli Wei,[†] Imhoi Koo,[†] Robin H. Schmidt,[‡,§] Xinmin Yin,[†] Seong Ho Kim,[¶] Andrew Vaughn,[∥] Craig J. McClain,[‡,§,∥,⊥] Gavin E. Arteel,[‡,§] Xiang Zhang,[†,#] and Walter H. Watson*[,‡,§,∥,#]

Departments of [†]Chemistry, [‡]Pharmacology & Toxicology, [§]Alcohol Research Center, and [∥]Medicine, University of Louisville, Louisville, Kentucky 40292, United States

[⊥]Robley Rex VAMC, Louisville, Kentucky 40292, United States

[¶]Biostatistics Core, Karmanos Cancer Institute, Wayne State University School of Medicine, Detroit, Michigan 48201, United States

Supporting Information

ABSTRACT: Arsenic is a widely distributed environmental component that is associated with a variety of cancer and non-cancer adverse health effects. Additional lifestyle factors, such as diet, contribute to the manifestation of disease. Recently, arsenic was found to increase inflammation and liver injury in a dietary model of fatty liver disease. The purpose of the present study was to investigate potential mechanisms of this diet−environment interaction via a high-throughput metabolomics approach. GC×GC−TOF MS was used to identify metabolites that were significantly increased or decreased in the livers of mice fed a Western diet (a diet high in fat and cholesterol) and co-exposed to arsenic-contaminated drinking water. The results showed that there are distinct hepatic metabolomic profiles associated with eating a high fat diet, drinking arsenic-contaminated water, and the combination of the two. Among the metabolites that were decreased when arsenic exposure was combined with a high fat diet were short-chain and medium-chain fatty acid metabolites and the anti-inflammatory amino acid, glycine. These results are consistent with the observed increase in inflammation and cell death in the livers of these mice and point to potentially novel mechanisms by which these metabolic pathways could be altered by arsenic in the context of diet-induced fatty liver disease.

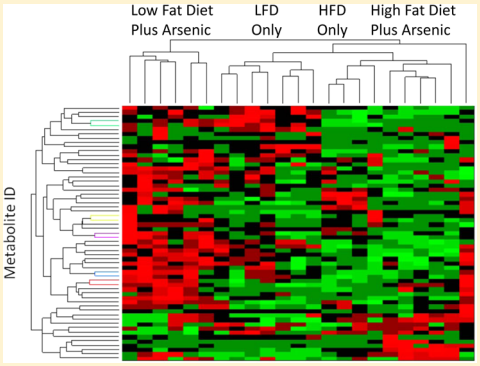

KEYWORDS: *GC×GC−TOF MS, metabolomics, liver, sodium arsenite, high fat diet*

1. INTRODUCTION

Diet−environment interactions play an important role in human disease. These interactions are particularly apparent in the development and progression of fatty liver disease. According to the prevailing two hit hypothesis,[1] dietary factors such as excessive fat consumption contribute to the formation of fatty liver, which makes the liver susceptible to a second hit which promotes the progression to more severe liver injury. Several factors have been shown to mediate the progression from simple steatosis (fatty liver) to steatohepatitis (fatty liver with inflammation and cell death),[2] and environmental agents that activate these factors can contribute to the extent of liver injury.[3,4] For example, arsenic was recently shown to contribute to the progression of diet-induced fatty liver disease by increasing inflammatory mediators in the livers of mice.[5]

Arsenic is a naturally occurring component of the Earth's crust, and groundwater concentrations can reach harmful levels in regions where arsenic is particularly abundant. Although there are several regions in the United States where municipal water supplies and private artesian wells have arsenic concentrations exceeding the Maximum Contaminant Level of 10 parts per billion (ppb) set by the World Health Organization and the Environmental Protection Agency, arsenic concentrations can reach much higher concentrations in places like Bangladesh and West Bengal.[6] Epidemiological studies in these highly exposed populations have revealed strong links between arsenic exposure and skin lesions, hypertension, cardiovascular disease, respiratory disease, and cancer.[7] In the liver, high arsenic exposure results in hepatomegaly, portal hypertension, non-cirrhotic portal fibrosis, and cancer.[8] It is unclear whether the liver is a primary target of toxicity in people exposed to lower levels of arsenic, such as those seen in the United States. It is more likely that the adverse effects of arsenic on the liver will depend on the presence of other sensitizing factors like fatty liver disease.

We recently reported that mice fed a diet high in fat and cholesterol (the so-called Western diet) for 10 weeks developed steatosis, while simultaneous exposure to drinking water contaminated with arsenic resulted in much more inflammation and cell death.[5] In that study, 5 parts per million (ppm) arsenic had no effect on the livers of mice fed a low fat control diet.

Received: July 11, 2013
Published: December 11, 2013

While this concentration is higher than those that produce hepatotoxicity in human populations,[8] the absorption, distribution, and metabolism of arsenic is much different in mice than in humans. Indeed, a recent report showed that it took 10 times higher concentrations of drinking water arsenic (50 ppm) to achieve liver arsenic concentrations similar to those seen in humans exposed to arsenic in West Bengal.[9]

To better understand the interactions between arsenic and diet-induced fatty liver disease, we employed high-throughput comprehensive two-dimensional gas chromatography time-of-flight mass spectrometry (GC×GC−TOF MS) to analyze liver metabolites altered by arsenic, a high fat diet, and the combination of the two. GC×GC−TOF MS is one of the most powerful analytical platforms for metabolomics analyses. It uses two capillary GC columns of different polarities connected via a thermal modulator to achieve a high degree of separation of metabolites.[10−12] Compared to the 15−60 m length of the first dimension column, the length of the second dimension column is very short, in general only 0.5−2 m. The analytes coeluted from the first column are further separated in the second column because of the difference of column temperature and the chromatographic polarities. The further separated analytes are directed to a high capacity time-of-flight mass spectrometry system for detection. The GC×GC−TOF MS platform offers significant advantages over other metabolomics platforms for analysis of complex samples, including an order-of-magnitude increase in separation capacity, significant increase in signal-to-noise ratio and dynamic range, and improvement of mass spectral deconvolution and similarity matches.[13,14]

2. MATERIALS AND METHODS

2.1. Animals and Diets

Four-week-old male C57BL/6J mice were purchased from The Jackson Laboratory (Bar Harbor, ME). Mice were housed in a pathogen-free barrier facility accredited by the Association for Assessment and Accreditation of Laboratory Animal Care. Food and tap water were allowed ad libitum. The procedures of animal care were approved by the University of Louisville Institutional Animal Care and Use Committee.

All mice were fed AIN-76A Purified diet (Harlan Laboratories, Madison, WI) for 1 week to minimize the potential confounding factor of arsenic present in standard laboratory chow.[15] At 5 weeks of age, mice were exposed to sodium arsenite (5 ppm in tap water) or tap water for 1 week prior to initiating feeding with either low fat diet (LFD; 13% of calories from fat) or high fat diet (HFD; 42% of calories from fat) (diets TD.08485 and TD.88137, Harlan Laboratories, Madison, WI) for 10 weeks. This exposure level of arsenic was shown in our previous study[5] to cause no overt liver damage in mice fed a low fat diet but to exacerbate liver injury induced by a high fat diet. Four different treatment groups were evaluated in this study: 6 mice fed a low fat diet and tap water (sample group LFD); 6 mice fed a low fat diet and tap water containing sodium arsenite (sample group LFD+As); 5 mice fed a high fat diet and tap water (sample group HFD); 6 mice fed a high fat diet and tap water containing sodium arsenite (sample group HFD+As). Food and water consumption were measured twice a week. Body weight was measured once a week. For termination, mice were anesthetized with ketamine/xylazine (100/15 mg/kg i.m.). Portions of liver tissue were frozen immediately in liquid nitrogen.

2.2. Metabolite Sample Preparation

A sample of liver tissue was weighed and then homogenized for 2 min after adding water at a ratio of 100 mg liver tissue/mL water. The homogenized sample was then stored at −80 °C until use. A 100-μL aliquot of the homogenized liver sample and 400 μL of methanol were mixed and vortexed for 1 min followed by centrifugation at room temperature for 10 min at 15000 rpm. Then 400 μL of the supernatant was aspirated into a plastic tube and dried by N_2 flow. The metabolites extracts were then dissolved in 40 μL of ethoxyamine hydrochloride solution (30 mg/mL) and vigorously vortex-mixed for 1 min. Methoxymation was carried out at 70 °C for 1 h. After adding 40 μL of *N*-(*tert*-butyldimethylsilyl)-*N*-methyltrifluoroacetamide (MTBSTFA) mixed with 1% *tert*-butyldimethylchlorosilane (TBDMSCI), derivatization was carried out at 70 °C for 1 h. Stock solutions were then transferred to GC vials for analysis. The methoxymation and derivatization were prepared just before GC×GC−TOF MS analysis.

2.3. GC×GC−TOF MS Analysis

A LECO Pegasus 4D GC×GC−TOF MS instrument was equipped with an Agilent 6890 gas chromatograph and a Gerstel MPS2 autosampler (GERSTEL Inc., Linthicum, MD), featuring a LECO two-stage cryogenic modulator and secondary oven. The primary column was a 60 m × 0.25 mm ${}^1d_c$ × 0.25 μm ${}^1d_f$, DB-5 ms GC capillary column (phenyl arylene polymer virtually equivalent to (5%-phenyl)-methylpolysiloxane). A second GC column of 1 m × 0.25 mm ${}^1d_c$ × 0.25 μm ${}^2d_f$, DB17 ms ((50%-phenyl)-methylpolysiloxane) was placed inside the secondary GC oven after the thermal modulator. Both columns were obtained from Agilent Technologies (Agilent Technologies J&W, Santa Clara, CA). The helium carrier gas (99.999% purity) flow rate was set to 1.0 mL/min at a corrected constant flow via pressure ramps. The inlet temperature was set at 280 °C. The primary column temperature was programmed with an initial temperature of 60 °C for 0.5 min, then ramped at 5 °C/min to 280 °C, and maintained for 12 min. The secondary column temperature program was set to an initial temperature of 70 °C for 0.5 min and then also ramped at the same temperature gradient employed in the first column to 280 °C, accordingly. The thermal modulator was set to +20 °C relative to the primary oven, and a modulation time of P_M = 2.5 s was used. The mass range was set as 45−1000 m/z with an acquisition rate of 200 mass spectra per second. The ion source chamber was set at 230 °C with the transfer line temperature of 280 °C, and the detector voltage was 1680 V with electron energy of 70 eV. The acceleration voltage was turned on after a solvent delay of 775 s. The split ratio was set at 40:1.

2.4. Data Analysis

The GC×GC−TOF MS data were processed using LECO's instrument control software ChromaTOF for peak picking and tentative metabolite identification, followed by retention index matching, peak merging, peak list alignment, normalization, and statistical significance test.[16] For metabolite identification using ChromaTOF, each chromatographic peak was tentatively assigned to a metabolite if its experimental mass spectrum and a database spectrum have a spectral similarity score no less than 600. Note that the maximum spectral similarity score is 1000. Peak merging and peak list alignment were carried out using DISCO software,[17] while the retention index matching was performed using iMatch software with the *p*-value threshold set as $p \leq 0.001$.[18] The pairwise two-tail *t* test was

used to determine whether a metabolite has a significant abundance difference between sample groups by setting the threshold of false discovery rate (FDR) $q \leq 0.2$.

To further verify the identification of metabolites detected with significant abundance difference between sample groups, commercially available authentic standards of these metabolites were analyzed on GC×GC−TOF MS under the same experimental conditions as the biological samples analyzed. A tentative metabolite assignment was considered as a correct identification only if the experimental information of the authentic metabolite agreed with the corresponding information of the chromatographic peak in the biological samples, i.e., difference of the first dimension retention time ≤10 s, difference of the second dimension retention time ≤0.06 s, and the mass spectral similarity ≥700.

3. RESULTS

3.1. Metabolite Detection and Platform Accuracy

GC×GC−TOF MS instrument data provide four pieces of information for each metabolite: the first dimension retention time ^1t_R, the second dimension retention time ^2t_R, fragment ion m/z, and peak height of each fragment ion. The information of fragment ion m/z and peak height forms the mass spectrum of the metabolite. Figure 1 is a contour plot of the GC×GC−TOF MS data acquired from a sample randomly selected from the sample group LFD. The color of each data point is the signal intensity.

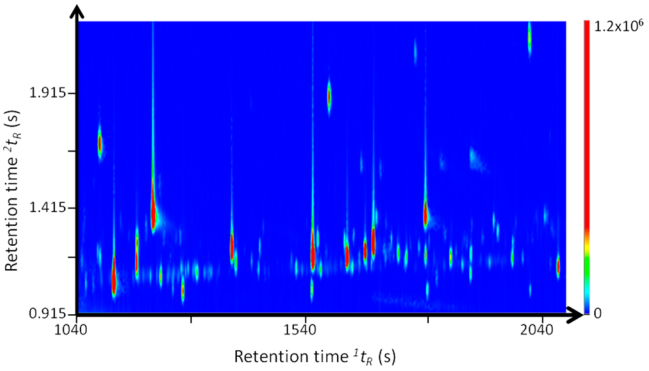

Figure 1. Sample GC×GC−TOF MS chromatograms of metabolite extract from mouse liver. The *x*-axis is the first dimension retention time ^1t_R in seconds. The *y*-axis is the second dimension retention time ^2t_R in seconds. The color bar shows the signal intensity of each peak plotted on the chromatogram in total ion current.

The instrument data were first processed using commercial software ChromaTOF for peak picking and initial compound identification using the vendor recommended parameters, and the information of the top 1500 abundant chromatographic peaks were reported. By setting the threshold of spectral similarity ≥600, about 570−730 chromatographic peaks were assigned to compounds in each sample, while the remaining chromatographic peaks were assigned as unknowns. The average peak area of the chromatographic peaks with initial identification results is about 6 times larger than the average peak area of the chromatographic peaks assigned as unknowns. The chromatographic peaks with positive identifications were further subjected for retention index matching using iMatch algorithm. By setting the threshold $p \leq 0.001$, about 380−520 compounds had correct retention index values in each sample, and the remaining chromatographic peaks were reassigned as unknowns. All retention index matched compounds were used for alignment using the DISCO algorithm. A total of 402 peaks were aligned. The aligned metabolites were further filtered by removing compounds detected in the blank samples as well as the compounds that detected in less than 75% of samples in each sample group. By doing so, about 100 metabolites were left between two sample groups for statistical significance test and FDR analysis.

The ability of the platform to accurately identify metabolites with significant abundance differences between two sample groups was assessed by spiking different concentrations of a mixture of standards into a sample. Details of the experiments are presented in Supporting Information and reported in ref 16. Supplemental Figure S1 shows the receiver operator curves produced by these spike-in experiments. A large value of area under curve (AUC) in the receiver operating characteristic (ROC) curve demonstrates that the analytical platform and the data analysis methods used in this study are effective in recognizing the metabolites with significant differences.

3.2. Metabolite Identification

Metabolite identification was done in three sequential steps in this study: mass spectral matching, retention index matching, and comparison with authentic standards. In general, about 570−730 chromatographic peaks were assigned to a metabolite name by ChromaTOF in one sample based on mass spectral matching. It is common that multiple distinct chromatographic peaks can be assigned to the same metabolite by mass spectral matching, due to limited accuracy of the identification algorithm.[13,14] For example, glycine, *N*-(*tert*-butyldimethylsilyl)-, *tert*-butylsimethylsilyl ester was assigned to three distinct chromatographic peaks with two-dimensional retention times of (1655 s, 1.155 s), (1845 s, 1.055 s), and (1850 s, 1.045 s), respectively. The spectral similarity of these three assignments to the mass spectra in the NIST11 database was 872, 731 and 787, respectively. In order to reduce the rate of false identification, we employed retention index matching to remove the false positive identifications. By setting the threshold $p \leq 0.001$ in iMatch software, the chromatographic peaks with the two-dimensional retention time values of (1845 s, 1.055 s) and (1850 s, 1.045 s) were recognized as false identifications and excluded from the downstream analysis, due to large retention index difference. Metabolite identifications based on retention index matching were further confirmed by comparison to authentic standards. Comparison with authentic standards was used to verify the identity of only the metabolites that were detected with significant abundance changes between sample groups. Mass spectral similarity and retention time variation were used when comparing metabolite peaks in biological samples to those of the authentic standards. For example, glycine was detected as a metabolite with significant abundance changes between sample groups HFD+As and HFD. The retention time values for the metabolite identified as glycine in the biological samples were (1655 s, 1.155 s). The authentic standard of glycine that was derivatized and analyzed on GC×GC−TOF MS under the same conditions as the biological samples eluted at ^1t_R = 1655 s and ^2t_R = 1.165 s, which is very similar to the peaks eluted in the biological sample with identical ^1t_R and a difference of 0.01 s in ^2t_R. The mass spectral similarity between the authentic standards and the biological sample was 970, demonstrating the correct identification of glycine from the biological samples.

dx.doi.org/10.1021/pr400719u | J. Proteome Res. 2014, 13, 547−554

Table 1. Metabolites in Mouse Liver with Significance Abundance Difference between Sample Groups HFD and LFD

metabolite	*p*-value	*q*-value	^1t_R (s)	^2t_R (s)	CAS no.	fold change[a]
tetradecanoic acid	1.4×10^{-2}	4.3×10^{-2}	2323.8	1.228	544-63-8	1.5
pentadecanoic acid	1.4×10^{-4}	1.3×10^{-3}	2432.6	1.243	1002-84-2	2.3
L-cysteine	3.0×10^{-5}	3.7×10^{-4}	2440.0	1.262	52-90-4	1.7
L-threonine	2.4×10^{-2}	5.2×10^{-2}	1900.5	1.208	72-19-5	2.1
L-lysine	5.2×10^{-4}	3.2×10^{-3}	2625.7	1.272	56-87-1	−2.5
pentanoic acid, 3-methyl-2-oxo-[b]	3.6×10^{-2}	6.6×10^{-2}	2205.1	1.363	1460-34-0	1.2
L-methionine	1.3×10^{-2}	4.3×10^{-2}	2177.5	1.280	63-68-3	1.4
L-glutamic acid	2.4×10^{-2}	5.2×10^{-2}	2510.0	1.244	56-86-0	1.5
taurine	3.8×10^{-6}	1.4×10^{-4}	2117.5	1.351	107-35-7	4.5

[a]The sample group LFD is the reference group. "+" sign refers to abundance increase in sample group HFD, while " −" sign refers to abundance decrease in sample group HFD. [b]Tentative identification without technical verification using authentic standards.

Some metabolites tentatively assigned by mass spectrum matching and retention index filtering were not compared to authentic standards because they were not available in our laboratory. Because this technical verification was not performed, their identification remained tentative. Tentatively identified metabolites were considered as false identifications and removed from the identification list, if they were recognized as drugs or from non-mammalian animals during metabolic network analysis by the Ingenuity Pathway Analysis (IPA) software (Ingenuity Systems, Inc., Redwood City, CA). The remaining tentatively identified metabolites were included in subsequent analyses but have been labeled as tentative in Tables 1−3.

3.3. Metabolite Quantification

To study the abundance change of a metabolite between two testing sample groups, the pairwise two-tail *t* test was employed by setting the threshold of false discovery rate as $q \leq 0.2$. The term fold change was defined as the ratio of the large abundance value (peak area) of a metabolite in one group divided by the small abundance value of the same metabolite in the other group. A positive sign and a negative sign indicate the abundance increase and decrease in the testing sample group compared to the reference sample group, respectively.

Figure 2 depicts a sample abundance distribution of metabolite glycine in sample groups HFD and HFD+As. Glycine was detected by the statistical significance test as one of the metabolites that have significant abundance changes between these two sample groups. Compared with its abundance in the HFD group, glycine is 1.7-fold lower in the HFD+As group with a *p*-value of 5.0×10^{-3}.

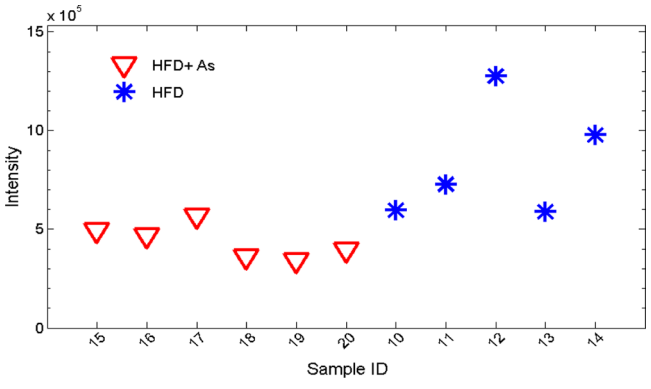

Figure 2. Abundance distribution of metabolite glycine in the liver samples of HFD+As group and HFD group. The abundance test (pairwise two-tail *t* test) shows that the regulation of this metabolite in the HFD+As group is decreased with a fold change of 1.7 and a *p*-value of 5.0×10^{-3} comparing with HFD group.

Mice fed a high fat diet develop steatotosis.[5] To establish the metabolomic changes that accompany this liver injury, the metabolites with significant differences in abundance between the HFD group and the LFD group were determined (Table 1). Eight metabolites were increased and one metabolite was decreased in the HFD group relative to the LFD group. As would be expected when comparing mice fed a diet high in fat to mice fed a low fat diet, two of the increased metabolites were fatty acids, whereas none of the decreased metabolites were fatty acids.

Table 2 shows the effects of arsenic in mice fed the low fat diet (LFD+As vs LFD). There were no signs of liver injury in either of these groups, but there were significant metabolic differences resulting from arsenic exposure. The abundance of one metabolite was decreased, while seven metabolites were increased in the LFD+As group compared to the LFD group. Three fatty acids were detected with significant regulation changes by arsenic. The levels of two fatty acids were increased, while one was decreased.

Table 3 presents the results of arguably the most important comparison in this study: the metabolic differences between the HFD and HFD+As groups. Whereas the HFD produces mild liver injury in the form of steatosis, co-exposure to arsenic results in even more severe liver injury, with elevated markers of inflammation and cell death.[5] The combination of arsenic and a high fat diet (HFD+As) resulted in abundance changes in nine metabolites relative to the effect of a high fat diet alone (HFD), with six metabolites decreasing and three metabolites increasing. The metabolites that were lower in the HFD+As group were short-chain fatty acids, medium-chain fatty acids, the two acidic amino acids aspartate and glutamate, and the anti-inflammatory amino acid glycine. The metabolites that were higher in the HFD+As group were the amino acids cysteine and lysine and the citric acid cycle intermediate, citric acid. Additional between-group comparisons are provided in the Supporting Information as Tables S1 and S2.

4. DISCUSSION

Multiple data analysis steps were involved in analysis of the GC×GC−TOF MS data in this study. In order to control the false discovery rate, the experimental data were analyzed using different values of FDR threshold including $q \leq 0.05$, 0.1, 0.15, 0.2, and 0.3. The numbers of metabolites detected with significant abundance change between two sample groups are listed in Supporting Information as Table S3. It is generally known that the statistical power increases as the FDR increases

dx.doi.org/10.1021/pr400719u | J. Proteome Res. 2014, 13, 547−554

Table 2. Metabolites in Mouse Liver with Significance Abundance Difference between Sample Groups LFD+As and LFD

metabolite	*p*-value	*q*-value	^1t_R (s)	^2t_R (s)	CAS no.	fold change[a]
heptanoic acid	4.7×10^{-3}	4.2×10^{-2}	1397.5	1.158	111-14-8	−1.4
dodecanoic acid	3.5×10^{-3}	4.2×10^{-2}	2089.3	1.204	143-07-7	1.7
pentadecanoic acid	3.3×10^{-2}	9.8×10^{-2}	2432.6	1.243	1002-84-2	1.3
L-proline	1.2×10^{-2}	5.1×10^{-2}	1935.1	1.235	147-85-3	1.2
L-cysteine	3.0×10^{-2}	9.6×10^{-2}	2440.0	1.262	52-90-4	1.3
L-methionine	3.0×10^{-3}	4.2×10^{-2}	2177.5	1.280	63-68-3	1.4
GABA (4-aminobutanoic acid)[b]	8.4×10^{-3}	5.0×10^{-2}	1926.5	1.188	56-12-2	1.5
pentanoic acid, 3-methyl-2-oxo-[b]	2.3×10^{-3}	4.2×10^{-2}	2205.1	1.363	1460-34-0	1.8

[a]The sample group LFD is the reference group. "+" sign refers to abundance increase in sample group LFD+As, while " −" sign refers to abundance decrease in sample group LFD+As. [b]Tentative identification without technical verification using authentic standards.

Table 3. Metabolites in Mouse Liver with Significance Abundance Difference between Sample Groups HFD+As and HFD

name	*p*-value	*q*-value	^1t_R (s)	^2t_R (s)	CAS no.	fold change[a]
dodecanoic acid	4.8×10^{-2}	1.1×10^{-1}	2089.3	1.204	143-07-7	−1.3
glycine	5.0×10^{-3}	3.0×10^{-2}	1655.0	1.159	56-40-6	−1.7
α-aminoisobutyric acid[b]	3.4×10^{-2}	1.1×10^{-1}	1686.9	1.166	62-57-7	−1.6
L-glutamic acid	4.2×10^{-3}	2.8×10^{-3}	2510.0	1.244	56-86-0	−1.4
2-hydroxybutyric acid	4.9×10^{-2}	1.1×10^{-1}	1642.4	1.135	600-15-7	−1.4
L-aspartic acid	4.6×10^{-2}	1.1×10^{-1}	2385.0	1.225	56-84-8	−1.2
L-cysteine	1.5×10^{-2}	5.8×10^{-2}	2440.0	1.262	52-90-4	1.4
citric acid[b]	3.3×10^{-2}	1.1×10^{-1}	2911.1	1.593	77-92-9	1.7
L-lysine	6.0×10^{-2}	1.3×10^{-1}	2625.7	1.272	56-87-1	1.7

[a]The sample group HFD is the reference group. "+" sign refers to abundance increase in sample group HFD+As, while " −" sign refers to abundance decrease in sample group HFD+As. [b]Tentative identification without technical verification using authentic standards.

at a fixed sample size, while the power increases as the sample size increases at a fixed FDR.[17] Consequently, a larger FDR threshold is required to achieve a desirable power when the sample size is small. For this reason, we selected $q \leq 0.2$ to achieve a reasonable power due to the small sample size in this study. Figure S2 in Supporting Information depicts the clustering results of the four sample groups.

The results presented here demonstrate that both high dietary fat intake and environmental arsenic exposure exert effects on liver metabolism and that the combination of the two exposures yields a unique metabolite profile that may offer some insight into the mechanisms of liver injury. Previously, we showed that mice fed the so-called Western diet (a diet high in milk fat and cholesterol) for 10 weeks gained more weight and had significantly more fat in their livers than mice fed a low fat diet,[5] consistent with other studies using this diet.[18,19] Importantly, co-exposure to arsenic-containing drinking water resulted in significantly greater inflammatory liver injury in this model,[5] suggesting that arsenic may be a second hit that promotes progression from steatosis to steatohepatitis.[1]

In the context of the two hit hypothesis of steatohepatitis,[1] one should consider how the metabolic changes elicited by the first hit (high fat diet) are affected by the second hit (arsenic). The high fat diet significantly altered nine metabolites (Table 1), and the addition of arsenic resulted in further alterations in three of these metabolites (Table 3). The HFD-induced increase in cysteine was amplified, whereas the increase in glutamate was blocked, by co-exposure to arsenic. Also, the HFD-induced decrease in lysine was reversed by arsenic. Furthermore, six additional metabolites were changed by the combination of the high fat diet and arsenic that were not altered by the high fat diet alone. Among these, glycine was decreased by the combination of arsenic and a high fat diet. Therefore, all three of the amino acids that constitute the antioxidant glutathione (glutamate, cysteine, and glycine) were altered, with glutamate and glycine levels lower and cysteine levels higher. Under normal conditions, cysteine concentrations are near the K_m for the rate-limiting enzyme glutathione synthesis,[20] and an increase in cysteine would be expected to increase the rate of synthesis. Indeed, Santra et al. reported that mice exposed to arsenic for 8 weeks had elevated levels of hepatic glutathione.[21] Thus, arsenic exposure may evoke a compensatory increase in glutathione synthesis in the liver, at least in response to these relatively short exposures. The increase in cysteine observed in the current study could reflect increased uptake of this rate-limiting amino acid in an attempt by the liver to compensate for an increased demand for glutathione synthesis. Cysteine is taken up by the cystine/glutamate antiporter, which exchanges extracellular cystine for intracellular glutamate.[22] The expression of this transporter is induced by oxidants, electrophiles, and inflammatory mediators.[22] Therefore, the increase in cysteine and decrease in glutamate observed in the present study may reflect increased activity of this transporter.

In addition to altered glycine, alterations in five other metabolites were specific to the HFD+As group. Three of these were fatty acids or fatty acid metabolites, and each of these was found to be decreased relative to the high fat diet alone. The high fat diet used in this study contained 21% (w/w) milk fat. The major fatty acids found in milk fat are palmitic acid (C16:0, 30% of the fatty acids), stearic acid (C18:0, 12%), myristic acid (C14:0, 11%), and lauric acid (C12:0, 3.3%).[23] We observed an increase in myristic acid in the livers of mice fed a high milk fat diet when compared to the mice fed the low fat control diet, but not palmitic, stearic, or lauric acids.

Interestingly, when mice were co-exposed to arsenic and a high fat diet, there was a decline in hepatic lauric acid levels. Diets high in saturated medium chain fatty acids, such as lauric

dx.doi.org/10.1021/pr400719u | J. Proteome Res. 2014, 13, 547−554

acid, protect against inflammatory liver injury caused by chronic alcohol ingestion[24,25] or acute endotoxin administration.[26] Recently, in a model of non-alcoholic fatty liver disease where rats were fed diets supplying 70% of calories from fat, replacing fat from corn oil with fats enriched in medium-chain triglycerides decreased steatosis and liver injury.[27] The mechanisms by which medium-chain lipids in general and lauric acid in particular inhibit inflammatory liver injury are not clear. In fact, some in vitro studies have found that lauric acid can be pro-inflammatory. For example, lauric acid increased inflammatory cytokine production by astrocytes and macrophages via activation of TLR4 signaling[28,29] but had no effect on cytokine production by adipocytes or endothelial cells.[30,31] It is possible that hepatic lauric acid contributes to inflammatory liver injury independently of any effects on cytokine production; its levels may influence responses to cytokines, or it may be a marker of alterations in other critical pathways such as mitochondrial fatty acid oxidation.[32] Additional studies will be needed to determine how arsenic and a high fat diet contribute to the down-regulation of lauric acid, and whether this down-regulation contributes to increased inflammation and/or injury in this model.

Two other fatty acid metabolites were decreased in the livers of mice fed arsenic and a high fat diet: 2-hydroxybutyrate and 2-aminobutyrate. Both of these compounds can be produced by the catabolism of threonine, and 2-hydroxybutyrate can also be formed in the conversion of methionine to cysteine in the transsulfuration pathway. A decrease in serum 2-hydroxybutyrate was recently reported in children with cystic fibrosis,[33] a disease associated with increased inflammation. It remains to be determined whether decreases in these metabolites are common to early stages of inflammatory tissue injury.

The decrease in glycine in the HFD+As group relative to the HFD group may be an important clue as to the mechanism by which the combination of arsenic and a high fat diet leads to inflammatory liver injury. Glycine supplementation protects the liver in a number of inflammatory injury models[34,35] by acting on glycine-gated chloride channels on Kupffer cells to inhibit inflammatory cytokine production.[34,36,37] The glycine deficiency in our model may have promoted pro-inflammatory signaling. In support of this, we observed a dramatic increase in the number of activated Kupffer cells, as determined by F4/80 staining, in response to arsenic exposure in the HFD group.[5]

It is unclear how arsenic and a high fat diet deplete hepatic glycine, but altered glycine metabolism could play a role. Threonine dehydratase is inhibited by cysteine,[38] which is elevated by arsenic and a high fat diet, both alone and in combination. Serine hydroxymethyltransferase has an active site cysteine as well as two closely spaced (vicinal) surface-exposed cysteines that can alter activity when modified by sulfhydryl reagents.[39,40] Arsenic binds to vicinal dithiols,[41] but it is not known whether serine hydroxymethyltransferase is a target of arsenic binding.

Metabolomics is a powerful approach for the discovery of pathways altered by environmental and dietary exposures related to disease. When used to investigate the combined effects of a high fat diet and arsenic in producing fatty liver with inflammation and cell death, metabolomic analyses revealed significant changes in the metabolism of short-chain and medium-chain fatty acids, as well as alterations in the pathways producing the anti-inflammatory amino acid glycine. Further investigations into the mechanisms by which these pathways are altered and the specific roles they play in the progression of nonalcoholic fatty liver disease are warranted.

Metabolites in mouse liver can have very diverse chemical characteristics. In this work, metabolites were extracted by water and methanol. Most of the nonpolar metabolites were lost during this analytical step. The extracted metabolites were then analyzed on GC×GC−TOF MS. Even though the GC×GC−TOF MS has a large separation power, it may not be enough to resolve all metabolites, resulting in overlapping chromatographic peaks that introduces significant challenges for metabolite identification and quantification. In this work, metabolite identification was first achieved by matching the experimental mass spectra to the mass spectra recorded in the NIST mass spectral library. The incompleteness of the existing mass spectral library not only introduces a certain degree of false-positive identifications but also leaves a number of chromatographic peaks without any compound identification. All of these technical limitations in the current study prevent us from seeing the entire picture of the metabolite profile in mouse liver. Further studies such as using different extraction methods, combining both GC×GC−TOF MS and 2D LC-MS, and applying multiple mass spectral libraries for metabolite identification may provide more comprehensive results. Further studies with a larger sample size will be also necessary to confirm the results in this study.

5. CONCLUSIONS

GC×GC−TOF MS was used to identify metabolites that were significantly increased or decreased in the livers of mice fed a Western diet (a diet high in fat and cholesterol) and co-exposed to arsenic-contaminated drinking water, to investigate potential mechanisms of this diet−environment interaction. The results showed that there are distinct hepatic metabolomic profiles associated with eating a high fat diet, drinking arsenic-contaminated water, and the combination of the two. Among the metabolites that were decreased when arsenic exposure was combined with a high fat diet were hepatoprotective short-chain and medium-chain fatty acid metabolites and the anti-inflammatory amino acid glycine. These results are consistent with the observed increase in inflammation and cell death in the livers of these mice and point to potentially novel mechanisms by which these metabolic pathways could be altered by arsenic in the context of diet-induced fatty liver disease.

■ ASSOCIATED CONTENT

Supporting Information

Analysis of samples with spiked-in standards and additional group-to-group comparisons. This material is available free of charge via the Internet at http://pubs.acs.org.

■ AUTHOR INFORMATION

Corresponding Author

*E-mail: bert.watson@louisville.edu.

Author Contributions

#These authors contributed equally to this work.

Notes

The authors declare no competing financial interest.

■ ACKNOWLEDGMENTS

The authors thank Mrs. Marion McClain for reviewing this manuscript. This work was supported by the National Institutes

of Health [R21ES021311, R01GM087735, 1RC2AA019385, P01AA017103, P30AA019360, R01AA015970, R37AA010762, R01AA018016, R01AA018869, R01DK071765, and R01AA018844] and the Veterans Administration.

REFERENCES

(1) Day, C. P.; James, O. F. Steatohepatitis: a tale of two "hits"? *Gastroenterology* **1998**, *114* (4), 842–5.
(2) Tilg, H.; Moschen, A. R. Evolution of inflammation in nonalcoholic fatty liver disease: the multiple parallel hits hypothesis. *Hepatology* **2010**, *52* (5), 1836–46.
(3) Cave, M.; Deaciuc, I.; Mendez, C.; Song, Z.; Joshi-Barve, S.; Barve, S.; McClain, C. Nonalcoholic fatty liver disease: predisposing factors and the role of nutrition. *J. Nutr. Biochem.* **2007**, *18* (3), 184–95.
(4) Wahlang, B.; Beier, J. I.; Clair, H. B.; Bellis-Jones, H. J.; Falkner, K. C.; McClain, C. J.; Cave, M. C. Toxicant-associated Steatohepatitis. *Toxicol. Pathol.* **2013**, *41* (2), 343–60.
(5) Tan, M.; Schmidt, R. H.; Beier, J. I.; Watson, W. H.; Zhong, H.; States, J. C.; Arteel, G. E. Chronic subhepatotoxic exposure to arsenic enhances hepatic injury caused by high fat diet in mice. *Toxicol. Appl. Pharmacol.* **2011**, *257* (3), 356–64.
(6) Argos, M.; Kalra, T.; Rathouz, P. J.; Chen, Y.; Pierce, B.; Parvez, F.; Islam, T.; Ahmed, A.; Rakibuz-Zaman, M.; Hasan, R.; Sarwar, G.; Slavkovich, V.; van Geen, A.; Graziano, J.; Ahsan, H. Arsenic exposure from drinking water, and all-cause and chronic-disease mortalities in Bangladesh (HEALS): a prospective cohort study. *Lancet* **2010**, *376* (9737), 252–8.
(7) Waalkes, M. P.; Liu, J.; Chen, H.; Xie, Y.; Achanzar, W. E.; Zhou, Y. S.; Cheng, M. L.; Diwan, B. A. Estrogen signaling in livers of male mice with hepatocellular carcinoma induced by exposure to arsenic in utero. *J. Natl. Cancer Inst.* **2004**, *96* (6), 466–74.
(8) Mazumder, D. N. Effect of chronic intake of arsenic-contaminated water on liver. *Toxicol. Appl. Pharmacol.* **2005**, *206* (2), 169–75.
(9) States, J. C.; Singh, A. V.; Knudsen, T. B.; Rouchka, E. C.; Ngalame, N. O.; Arteel, G. E.; Piao, Y.; Ko, M. S. Prenatal arsenic exposure alters gene expression in the adult liver to a proinflammatory state contributing to accelerated atherosclerosis. *PLoS One* **2012**, *7* (6), e38713.
(10) Ralston-Hooper, K.; Hopf, A.; Oh, C.; Zhang, X.; Adamec, J.; Sepulveda, M. S. Development of GC×GC/TOF-MS metabolomics for use in ecotoxicological studies with invertebrates. *Aquat. Toxicol.* **2008**, *88* (1), 48–52.
(11) Mohler, R. E.; Dombek, K. M.; Hoggard, J. C.; Pierce, K. M.; Young, E. T.; Synovec, R. E. Comprehensive analysis of yeast metabolite GC x GC-TOFMS data: combining discovery-mode and deconvolution chemometric software. *Analyst* **2007**, *132* (8), 756–67.
(12) Huang, X.; Regnier, F. E. Differential metabolomics using stable isotope labeling and two-dimensional gas chromatography with time-of-flight mass spectrometry. *Anal. Chem.* **2008**, *80* (1), 107–14.
(13) Kim, S.; Koo, I.; Jeong, J.; Wu, S.; Shi, X.; Zhang, X. Compound identification using partial and semipartial correlations for gas chromatography-mass spectrometry data. *Anal. Chem.* **2012**, *84* (15), 6477–87.
(14) Koo, I.; Zhang, X.; Kim, S. Wavelet- and Fourier-transform-based spectrum similarity approaches to compound identification in gas chromatography/mass spectrometry. *Anal. Chem.* **2011**, *83* (14), 5631–8.
(15) Kozul, C. D.; Nomikos, A. P.; Hampton, T. H.; Warnke, L. A.; Gosse, J. A.; Davey, J. C.; Thorpe, J. E.; Jackson, B. P.; Ihnat, M. A.; Hamilton, J. W. Laboratory diet profoundly alters gene expression and confounds genomic analysis in mouse liver and lung. *Chem. Biol. Interact.* **2008**, *173* (2), 129–40.
(16) Wei, X.; Shi, X.; Koo, I.; Kim, S.; Schmidt, R. H.; Arteel, G. E.; Watson, W. H.; McClain, C.; Zhang, X. MetPP: a computational platform for comprehensive two-dimensional gas chromatography time-of-flight mass spectrometry-based metabolomics. *Bioinformatics* **2013**, *29* (14), 1786–92.
(17) Tong, T.; Zhao, H. Practical guidelines for assessing power and false discovery rate for a fixed sample size in microarray experiments. *Stat. Med.* **2008**, *27* (11), 1960–72.
(18) Sydor, S.; Gu, Y.; Schlattjan, M.; Bechmann, L. P.; Rauen, U.; Best, J.; Paul, A.; Baba, H. A.; Sowa, J. P.; Gerken, G.; Canbay, A. Steatosis does not impair liver regeneration after partial hepatectomy. *Lab. Invest.* **2013**, *93* (1), 20–30.
(19) Shi, X.; Wahlang, B.; Wei, X.; Yin, X.; Falkner, K. C.; Prough, R. A.; Kim, S. H.; Mueller, E. G.; McClain, C. J.; Cave, M.; Zhang, X. Metabolomic analysis of the effects of polychlorinated biphenyls in nonalcoholic fatty liver disease. *J. Proteome Res.* **2012**, *11* (7), 3805–15.
(20) Lu, S. C. Glutathione synthesis. *Biochim. Biophys. Acta* **2013**, *1830* (5), 3143–53.
(21) Santra, A.; Maiti, A.; Chowdhury, A.; Mazumder, D. N. Oxidative stress in liver of mice exposed to arsenic-contaminated water. *Indian J. Gastroenterol.* **2000**, *19* (3), 112–5.
(22) Lewerenz, J.; Hewett, S. J.; Huang, Y.; Lambros, M.; Gout, P. W.; Kalivas, P. W.; Massie, A.; Smolders, I.; Methner, A.; Pergande, M.; Smith, S. B.; Ganapathy, V.; Maher, P. The cystine/glutamate antiporter system x(c)(-) in health and disease: from molecular mechanisms to novel therapeutic opportunities. *Antioxid. Redox Signaling* **2013**, *18* (5), 522–55.
(23) Ohlsson, L. Dairy products and plasma cholesterol levels. *Food Nutr. Res.* **2010**, 54.
(24) Kirpich, I. A.; Feng, W.; Wang, Y.; Liu, Y.; Barker, D. F.; Barve, S. S.; McClain, C. J. The type of dietary fat modulates intestinal tight junction integrity, gut permeability, and hepatic toll-like receptor expression in a mouse model of alcoholic liver disease. *Alcohol.: Clin. Exp. Res.* **2012**, *36* (5), 835–46.
(25) Nanji, A. A.; Jokelainen, K.; Tipoe, G. L.; Rahemtulla, A.; Dannenberg, A. J. Dietary saturated fatty acids reverse inflammatory and fibrotic changes in rat liver despite continued ethanol administration. *J. Pharmacol Exp. Ther.* **2001**, *299* (2), 638–44.
(26) Kono, H.; Fujii, H.; Asakawa, M.; Yamamoto, M.; Matsuda, M.; Maki, A.; Matsumoto, Y. Protective effects of medium-chain triglycerides on the liver and gut in rats administered endotoxin. *Ann. Surg.* **2003**, *237* (2), 246–55.
(27) Ronis, M. J.; Baumgardner, J. N.; Sharma, N.; Vantrease, J.; Ferguson, M.; Tong, Y.; Wu, X.; Cleves, M. A.; Badger, T. M. Medium chain triglycerides dose-dependently prevent liver pathology in a rat model of non-alcoholic fatty liver disease. *Exp. Biol. Med. (Maywood)* **2013**, *238* (2), 151–62.
(28) Gupta, S.; Knight, A. G.; Keller, J. N.; Bruce-Keller, A. J. Saturated long-chain fatty acids activate inflammatory signaling in astrocytes. *J. Neurochem.* **2012**, *120* (6), 1060–71.
(29) Huang, S.; Rutkowsky, J. M.; Snodgrass, R. G.; Ono-Moore, K. D.; Schneider, D. A.; Newman, J. W.; Adams, S. H.; Hwang, D. H. Saturated fatty acids activate TLR-mediated proinflammatory signaling pathways. *J. Lipid Res.* **2012**, *53* (9), 2002–13.
(30) Murumalla, R. K.; Gunasekaran, M. K.; Padhan, J. K.; Bencharif, K.; Gence, L.; Festy, F.; Cesari, M.; Roche, R.; Hoareau, L. Fatty acids do not pay the toll: effect of SFA and PUFA on human adipose tissue and mature adipocytes inflammation. *Lipids Health Dis.* **2012**, *11*, 175.
(31) Harvey, K. A.; Walker, C. L.; Pavlina, T. M.; Xu, Z.; Zaloga, G. P.; Siddiqui, R. A. Long-chain saturated fatty acids induce pro-inflammatory responses and impact endothelial cell growth. *Clin. Nutr.* **2010**, *29* (4), 492–500.
(32) Begriche, K.; Massart, J.; Robin, M. A.; Bonnet, F.; Fromenty, B. Mitochondrial adaptations and dysfunctions in nonalcoholic fatty liver disease. *Hepatology* **2013**, *58* (4), 1497–507.
(33) Joseloff, E.; Sha, W.; Bell, S. C.; Wetmore, D. R.; Lawton, K. A.; Milburn, M. V.; Ryals, J. A.; Guo, L.; Muhlebach, M. S. Serum metabolomics indicate altered cellular energy metabolism in children with cystic fibrosis. *Pediatr Pulmonol* **2013**, DOI: 10.1002/ppul.22859.

(34) Ikejima, K.; Iimuro, Y.; Forman, D. T.; Thurman, R. G. A diet containing glycine improves survival in endotoxin shock in the rat. *Am. J. Physiol.* **1996**, *271* (1 Pt 1), G97−103.
(35) Rose, M. L.; Germolec, D.; Arteel, G. E.; Schoonhoven, R.; Thurman, R. G. Dietary glycine prevents increases in hepatocyte proliferation caused by the peroxisome proliferator WY-14,643. *Chem. Res. Toxicol.* **1997**, *10* (10), 1198−204.
(36) Ikejima, K.; Qu, W.; Stachlewitz, R. F.; Thurman, R. G. Kupffer cells contain a glycine-gated chloride channel. *Am. J. Physiol.* **1997**, *272* (6 Pt 1), G1581−6.
(37) Wheeler, M. D.; Ikejema, K.; Enomoto, N.; Stacklewitz, R. F.; Seabra, V.; Zhong, Z.; Yin, M.; Schemmer, P.; Rose, M. L.; Rusyn, I.; Bradford, B.; Thurman, R. G. Glycine: a new anti-inflammatory immunonutrient. *Cell. Mol. Life Sci.* **1999**, *56* (9−10), 843−56.
(38) Leoncini, R.; Pagani, R.; Marinello, E.; Keleti, T. Double inhibition of L-threonine dehydratase by aminothiols. *Biochim. Biophys. Acta* **1989**, *994* (1), 52−8.
(39) Manohar, R.; Appaji Rao, N. Identification of active-site residues of sheep liver serine hydroxymethyltransferase. *Biochem. J.* **1984**, *224* (3), 703−7.
(40) Gavilanes, F.; Peterson, D.; Bullis, B.; Schirch, L. Structure and reactivity of cysteine residues in mitochondrial serine hydroxymethyltransferase. *J. Biol. Chem.* **1983**, *258* (21), 13155−9.
(41) Huang, C.; Yin, Q.; Zhu, W.; Yang, Y.; Wang, X.; Qian, X.; Xu, Y. Highly selective fluorescent probe for vicinal-dithiol-containing proteins and in situ imaging in living cells. *Angew. Chem., Int. Ed.* **2011**, *50* (33), 7551−6.